# COMPARATIVE STUDY OF HYDROXYAPATITE NANOCRYSTALS USING THE CHEMICAL PRECIPITATION AND HYDOTHERMAL TECHNIQUES

Supported by tetfund

**V. Ochigbo[1]*, M. O. Ochigbo-Ejembi[1], V. O. Ajibola[2], E. B. Agbaji[2], A. Giwa[3], P. Manivasakan[4], V. Rajendran[4]**
[1]National Research Institute for Chemical Technology (NARICT), Zaria-Nigeria
[2]Department of Chemistry, Ahmadu Bello University Zaria-Nigeria
[3]Department of Textile Science and Technology, Ahmadu Bello University Zaria-Nigeria
[4]Centre for Nano Science and Technology, KS Rangasamy College of Technology, Tiruchengode-637 215, Tamil Nadu India
*Corresponding author: ochigbovic@gmail.com

**Received:** March 13, 2019 **Accepted:** September 19, 2019

**Abstract:** Nano crystalline hydroxyapatite was prepared at physiological conditions of pH (7.4) and temperature (37ºC) by precipitation and hydrothermal methods using $Ca(NO_3).4H_2O$ and $NH_4H_2PO_4$ as precursors. The prepared samples were characterized via Particle size Analyser (PSA), Fourier transform infrared spectroscope (FT-IR), energy dispersive X-ray fluorescence (XRF/EDX), X-ray diffraction (XRD), Brunauer–EmmettTeller (BET), Scanning electron microscopy(SEM), Transmission electron microscopy (TEM) and Thermogravimetric/Differential thermal analyser (TG/DTA).The wet precipitated and hydrothermally synthesized crystals revealed Ca/P of 1.65 and 1.66, average particle size distribution of 26 and 29 nm specific surface area/ pore size/pore volume before and after calcination of (106 and 96 $m^2g^{-1}$/18 and 21.35 nm/0.65 and 0.48 $ccg^{-1}$) and (102 and 95 $m^2g^{-1}$/19.40 and 22.6 nm/0.62 and 0.43 $ccg^{-1}$), crystalline size (D)/ degree of crystallinity (Xc) of (5.03 nm/0.53) and (5.08 nm/1.82) a highly agglomerated uneven rod-like structures, respectively. The crystallinity/size and morphology as revealed by XRD and SEM were confirmed from the TEM images having sizes less than 100 nm and the crystalline nature of both powders. TG/DTA revealed the thermal stabilities of both powders beyond 800ºC.

**Keywords:** Comparative, hydroxyapatite, nanocrystals, physiological, precipitation hydrothermal

## Introduction

The resorption property of Calcium phosphates depends on Ca/P ratio, degreeofcrystallinity and crystal structure. A remarkable property of the synthetic hydroxyapatite (HA) is its bioactivity, in particular the ability to form chemical bonding with surrounding hard tissues after implantation (Fathi *et al*., 2008). However, most synthetic apatites are formed via high temperature processes, resulting in a well-crystallized structure, which has little or no activity toward bioresoption. To produce synthetic HA powders with the desired properties, wet-chemical methods (precipitation, hydrothermal technique, and hydrolysis of other calciumphosphate) and dry processes (solid-state reaction) can be used (Young and Holcomb, 1982).

Also, there were various techniques reported in literature for the production of nano-sized HA particles but none reports on its production at physiological conditions which is an integral part to its used as biomaterials; particularly, in these hydrothermal and precipitation techniques, moreover, there has been little attempt to investigate the effects of processing conditions on HA particle size, as the only processing variable reported is the effect of calcinations temperature on particle size (Feng *et al*., 2005; Fathi and Hanifi, 2007, 2008). So, the aim of this work is to synthesize and characterize a biomimetic Hydroxyapatite (HA) Nano-crystals via the hydrothermal and wet precipitation techniques at Physiological conditions while studying the effects of these processing parameters on the particle size and bioactivity.

## Materials and Methods

$Ca(NO_3)2{\cdot}4H_2O$ (98% MERCK), $NH_4H_2PO4$ (99% MERCK), $NH_4OH$ (25% MERCK) and ultrapure water (Arium 611UF; Sartorius AG) as the starting materials were used as received without any further purification.

### *The experimental procedures*

An aliquot (500ml) each of 0.5M of $Ca^{2+}$ and 0.3M of $HPO_4^{2-}$ precursors solutions prepared by dissolution of 118.075 g of $Ca(NO_3)_2.4H_2O$ and 34.509 g of $(NH_4)H_2PO_4$ in double distilled (DD) water in a beaker and transferred to 1000ml volumetric flasks, while the solutions were made to the mark were transferred into two separate beakers while the pH were respectively adjusted to physiological condition (7.4) using 25% $NH_4OH$ solution obtained by mixing of 25 ml of ammonia ($NH_3$) in 75 ml of water. To the beaker containing the $Ca^{2+}$ precursor solution, the $HPO_4^{2-}$ precursor solution was added drop wisely under continuous stirring at 200 rpm on a hot plate maintained at the temperature of 37ºC while constantly adjusting the pH while the mixture was vigorously stirred for 1hour under the same physiological conditions of pH and temperature. For the wet precipitation techniques, the thick milky gel produced was then aged at 37ºC for 24 h while for the hydrothermal technique, the thick milky gel produced was subsequently transferred into 125 ml Teflon-lined hydrothermal reactor (autoclave) and were then aged at 150ºC for 24 h in an air oven. The hydrothermal reactor was allowed to cool to room temperature. The resultant suspensions were centrifuged at 2000 rpm for 1 hour at 37ºC and filtered under mild suction and washed repeatedly with double distilled (DD) water and the residue dried at 80ºC for 24 h in an air oven. The resulting crystals were crushed into powder using mortar and pestle and calcinated at 300ºC for 3 h in a muffle furnace. Finally, both the calcined and uncalcined powders were then characterized using PSA, XRF/EDX, FT-IR, BET, XRD, SEM, TEM and TG/DTA.

## Results and Discussion

The chemical composition of the apatite (Table 1) from XRF/EDX studies confirmed the presence of calcium and phosphate in the apatite. Based on these XRF/EDX signatures, the Ca/P ratio of the hydroxyapatite obtained by the hydrothermal and wet precipitation methods were calculated as 1.66 and 1.65, respectively. The Ca/P ratios of HA powder obtained from the hydrothermal method appeared slightly higher compared to that obtained from the wet precipitation method, and this difference could be attributed to the elevated aging temperature which favours particle agglomeration, due to faster reaction that resulted to larger crystal formation and a more complex reaction with different phases of calcium phosphate formation under our experimental conditions, with respect to the wet precipitation method (Anita *et al.*, 2015).

The FT-IR spectra of the synthesized HA (Fig. 1 and Table 1) showed bands at 3572 and 631 $cm^{-1}$ corresponding to the hydroxyl group stretching and vibration modes respectively. The intense band at 962 $cm^{-1}$ corresponded to P–O stretching vibration modes whereas the doublet at 603 – 567 $cm^{-1}$ corresponds to O–P–O bending (Nejati *et al.*, 2009). Furthermore, the broad band at 3425 and 1640 $cm^{-1}$ were attributed to absorbed water, while the sharp bands at 3572 $cm^{-1}$ was attributed to the stretching vibration of the lattice OH. $PO_4^{3-}$ characteristics peaks appear at 568, 602, 962, 1040 and 1092 $cm^{-1}$. The observation of the asymmetric P–O stretching vibration of the $PO_4^{3-}$ band at 962 $cm^{-1}$ is a distinguishable band alongside the sharp bands at 633, 602, 568$cm^{-1}$, corresponding to the triply degenerate bending vibrations of $PO_4^{3-}$ in hydroxyapatite. Some $CO_3^{2-}$ derived bands were observed at 870 $cm^{-1}$ and around 1420-1480 $cm^{-1}$ indicating that a minute amount of carbonate substitution occurred (Elliot, 1994), which might be due to the adsorption of atmospheric carbon dioxide during the sample preparation, but, because carbonates are constituents of bone structures (Rajabi-Zamani *et al*., 2008) the presence of $CO_3^{2-}$ may play a vital role in the bioactivity of HA rather than being a cause of concern. The bands of absorbed water (H-O-H) around 1630 and 3450 $cm^{-1}$ appear narrower and sharper in the hydrothermal than the wet precipitation method. The band around 870 $cm^{-1}$ which corresponds to carbonate ion ($CO_3^{2-}$) group was more pronounced in the HA obtained by the wet precipitation than in the hydrothermal method. The band around 3572 $cm^{-1}$ which corresponds to the hydroxyl ion ($OH^-$) group appear sharper, with higher intensity for HA powder from the hydrothermal than the wet precipitation method. These variations in band intensities and appearance could be attributed to the elevated aging temperature of the hydrothermal method, otherwise all characteristic bands of the HA appeared similar in position. These results are in conformity with those reported by Nejati *et al.* (2009) using the same synthetic routes but different reaction temperatures.

From Fig. 1, the average particle size distribution (PSD) of the hydroxyapatite nanoparticles for the hydrothermal and wet precipitation methods were 29 nm ± 5% and 26 nm ± 5%, respectively, suggesting that greater percentage of these particle were within these sizes. Expectedly, the HA obtained by wet precipitation method had smaller particle size considering the particle size distribution, than the hydrothermal method, which by virtue of its higher temperature of aging should produce larger crystals, as hydrothermal treatment temperature can assist apatite crystal growth through provision of a highly active surface for the small apatite precipitate particles to bind to each other and grow into larger crystals compared to the wet precipitation where aging was done at ambient temperature (Zhang and Vecchio, 2007; Watanabe *et al*., 2009). Calcination of the HA powders resulted to a crystal with a decreased specific surface area (SSA) and pore volume (PV) with an increased pore size (PS), irrespective of the synthetic method (Table 2). This is attributable to the fact that Calcination increases the temperature of the crystal particle, which in turn leads to increase in particle size and the degree of agglomeration (Toledo-Antonio *et al*., 2003). Furthermore, there was a sharp decrease in SSA of the samples after calcinations. This sharp decrease in SSA of the samples after calcinations might be attributed to the presence of ammonia which might have enter the system during pH adjustment that was not completely washed during filtration\washing processes, and might also be due to the presence of chemically bonded water during the synthesis. HA crystals obtained by hydrothermal method had a smaller SSA and PV and an increased PS before and after calcination, compared to the HA obtained by wet precipitation method. The crystallite size (D) increases with calcination, as the hydrothermal method produced larger crystal sizes than the wet precipitation method, this difference observed could be attributed to the different aging temperatures. Comparing the average particle size ($D_A$) estimated by BET to the average crystallite size (D) estimated by XRD (Table 3), the average particle size calculated by BET was larger than the crystallite size calculated by XRD. This suggests that the particles contain several crystallites (Sergent *et al*., 2002).

**Table 1: Elemental compositions and Ca/P ratio of hydroxyapatite (HA) obtained at wet precipitation and hydrothermal methods**

| S/N | Elements (%) | Hydrothermal | Wet precipitation |
|---|---|---|---|
| 1 | Ca | 57.305 | 58.863 |
| 2 | P | 34.521 | 34.716 |
| 3 | Si | 7.788 | 6.384 |
| 4 | Fe | 0.7005 | 0.013 |
| 5 | Cu | 0.1995 | 0.010 |
| 6 | Sr | 0.1845 | 0.006 |
| | **Ca/P (%)** | **1.66** | **1.65** |

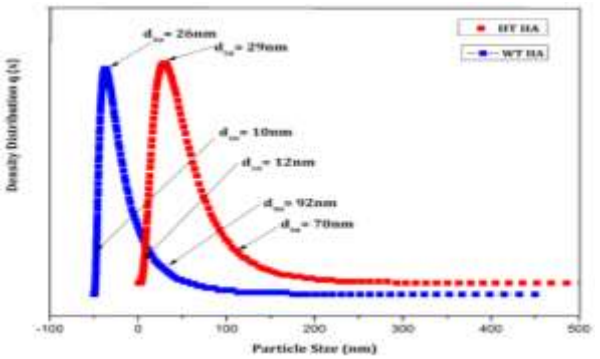


**Fig. 1: Particle size distribution of hydroxyapatite (HA) synthesized via hydrothermal (HT) and wet precipitation (WT)**

**Table 2: Specific surface area (SSA), pore size (PS), pore volume (PV) and average particle size ($D_A$) of hydroxyapatite (HA) before and after calcinations from BET analysis**

| S/N | Apatite (HA) | SSA($m^2$/g) | PV(nm) | PS(cc/g) | $D_A$(nm) |
|---|---|---|---|---|---|
| 1 | HA WT (A) | 106 | 0.65 | 18.67 | 17.91 |
| 2 | HA WT (B) | 96 | 0.48 | 21.32 | 19.77 |
| 3 | HA HT (A) | 102 | 0.62 | 19.40 | 18.61 |
| 4 | HA HT (B) | 95 | 0.43 | 22.60 | 19.98 |

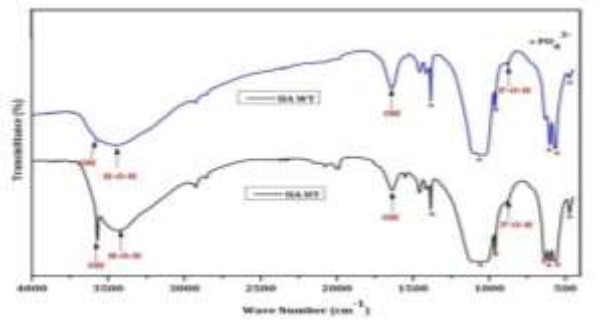

**Fig. 2:**FTIR spectra of HA synthesized via Hydrothermal (HT) & Wet precipitation (WT)

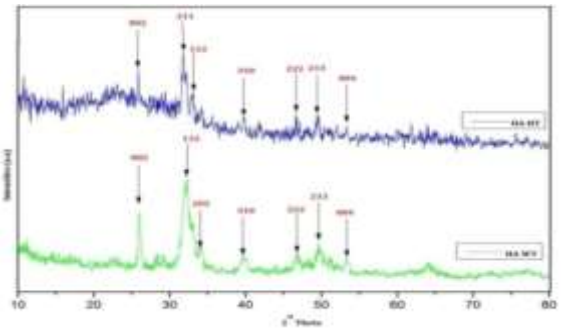

**Fig. 3: XRD pattern of HA synthesized via hydrothermal (HT) & wet precipitation (WT)**

From Fig. 1, the average particle size distribution (PSD) of the hydroxyapatite nanoparticles for the hydrothermal and wet precipitation methods were 29 nm ± 5% and 26 nm ± 5%, respectively, suggesting that greater percentage of these particle were within these sizes. Expectedly, the HA obtained by wet precipitation method had smaller particle size considering the particle size distribution, than the hydrothermal method, which by virtue of its higher temperature of aging should produce larger crystals, as hydrothermal treatment temperature can assist apatite crystal growth through provision of a highly active surface for the small apatite precipitate particles to bind to each other and grow into larger crystals compared to the wet precipitation where aging was done at ambient temperature (Zhang and Vecchio, 2007; Watanabe *et al*., 2009). Calcination of the HA powders resulted to a crystal with a decreased specific surface area (SSA) and pore volume (PV) with an increased pore size (PS), irrespective of the synthetic method (Table 2). This is attributable to the fact that Calcination increases the temperature of the crystal particle, which in turn leads to increase in particle size and the degree of agglomeration (Toledo-Antonio *et al*., 2003). Furthermore, there was a sharp decrease in SSA of the samples after calcinations. This sharp decrease in SSA of the samples after calcinations might be attributed to the presence of ammonia which might have enter the system during pH adjustment that was not completely washed during filtration\washing processes, and might also be due to the presence of chemically bonded water during the synthesis. HA crystals obtained by hydrothermal method had a smaller SSA and PV and an increased PS before and after calcination, compared to the HA obtained by wet precipitation method. The crystallite size (D) increases with calcination, as the hydrothermal method produced larger crystal sizes than the wet precipitation method, this difference observed could be attributed to the different aging temperatures. Comparing the average particle size ($D_A$) estimated by BET to the average crystallite size (D) estimated by XRD (Table 3), the average particle size calculated by BET was larger than the crystallite size calculated by XRD. This suggests that the particles contain several crystallites (Sergent *et al*., 2002).

Structural information on the apatite via XRD (Fig. 3) shows that, the hydrothermally prepared hydroxyapatite has major diffraction peaks located at 2θ = 25.7º(002), 2θ = 39.8º (310), 32.9º (300), 2θ = 46.7º (222), 2θ = 49.5º (213), 2θ = 53.4º (004), while HA obtained from wet precipitation had its major diffraction peaks at 2θ = 25.9º (002), 2θ = 32.2º(112), 2θ = 34.0º (202), 2θ = 39.7º(310), 2θ = 46.8º(222), 2θ = 49.5º(212), 2θ = 53.1º (004). These diffraction peaks when compared to standard peaks from the International Centre for Crystal Diffraction (ICCD), and literature values were found to be consistent and the predominant phase were confirmed as hydroxyapatite (HA) when matched with the Joint Committee for Powder Diffraction Standards (JCPDS), for calcium phosphates file number 00 – 009 – 0432. Furthermore, the crystallite size (D) and degree of crystallinity (Xc) were higher in the HA nanocrystals, obtained from the hydrothermal method than the wet precipitation method (Table 3). The lattice parameters (a and c) for the HA were 0.943 and 0.689 nm and 0.942 and 0.686 nm, respectively for the hydrothermal and wet precipitation methods. The crystallites size (D) and the degree of crystallinity ($X_c$) of the HA estimated using the Debye scherrer equation were found to be 5.08 and 1.81 nm for the hydrothermally prepared HA and 5.03 and 0.54 nm for HA prepared by wet precipitation (Table 3). This observation was supported by result of particle size distribution (PSD), where the HA obtained from the wet precipitation method has smaller average particle size distribution of 26 nm ± 5% to 29 nm ± 5% for the hydrothermal method. Comparing these average crystallite sizes (D) estimated by XRD to the average particle sizes ($D_A$) estimated by BET (Table 3), the average particle size calculated by BET was larger than the crystallite size calculated by XRD. This suggests that the particles contain several crystallites (Sergent *et al*., 2002).

**Table 3: The crystallite size (D), degree of crystallinity (Xc) and the lattice parameters of hydroxyapatite (HA) synthesized via hydrothermal and wet precipitation methods**

| Parameters/Methods | Crystal size parameters | | Crystal lattice parameters | | | |
|---|---|---|---|---|---|---|
| | Crystallite size D (nm) | Degree of crystallinity (Xc) | HA (Theoretical) a(nm) | HA (Theoretical) c(nm) | HA (Experimental) a(nm) | HA (Experimental) c(nm) |
| Wet Precipitation | 5.0316 | 0.5374 | 0.942 | 0.688 | 0.942 | 0.686 |
| Hydrothermal | 5.0812 | 1.8136 | 0.942 | 0.688 | 0.943 | 0.689 |

From the surface morphology of the HA, samples were examined using SEM analysis (Figs. 4 and 5), the hydrothermally synthesized HA showed a non-uniformly distributed rod like crystals, with high agglomeration (Fig 4) while the hydroxyapatite prepared by wet precipitation exhibited less agglomerated uneven structure crystals (Fig 5), with numerous spherical and plate like crystals that were agglomerated together to form rod like shape. The morphology for the wet precipitation method has a non-uniformed size of particle with various size distributions whereas the morphology of the hydrothermal method showed an obvious change with increasing average particle size and more agglomeration among the particles due to the elevated aging temperature.

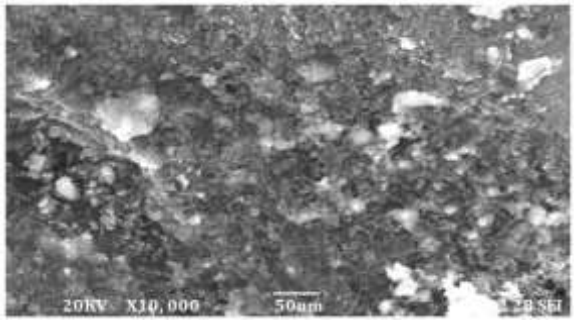


**Fig. 4: SEM Image of HA synthesized via hydrothermal (HT) method**

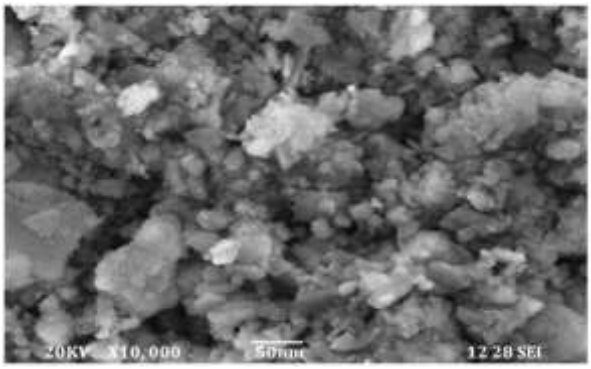


**Fig. 5: SEM image of HA synthesized via wet precipitation (WT) method**

The result from the Transmission Electron Microscope (TEM), indicated that all the particles exhibited a rod-like shape with varying degrees of agglomeration among fine particles, making the particles size difficult to measure. The image of HA from the hydrothermal method (Fig. 6) showed a closely agglomerated, non-uniform spherical nano particles, whereas the HA from the wet precipitation method (Fig. 7) showed less agglomerated particles, with non-uniform shapes. The hydrothermally prepared hydroxyapatite powder showed particles with high degree of agglomerationcaused by elevated aging temperature, which resulted to mutual interaction between particles arising from some forces like the Van-der-Waals forces, capillary forces and electrostatic forces (Pug and Bergstrom, 1994; Cukrov *et al*., 2001). This observation is consistent with those observed from the SEM micrographs and the result of Muthusamy *et al*. (2012). Furthermore, from the selected area electron diffraction (SAED) pattern, hydroxyapatite (HA) obtained by both the wet precipitation and the hydrothermal methods were characterized by diffraction rings, this suggests a fully crystallized nature of the apatite. However, in addition to the diffraction rings, the hydrothermally prepared hydroxyapatite has some discrete spots that indicate that it was fully crystallized with polycrystalline nature.

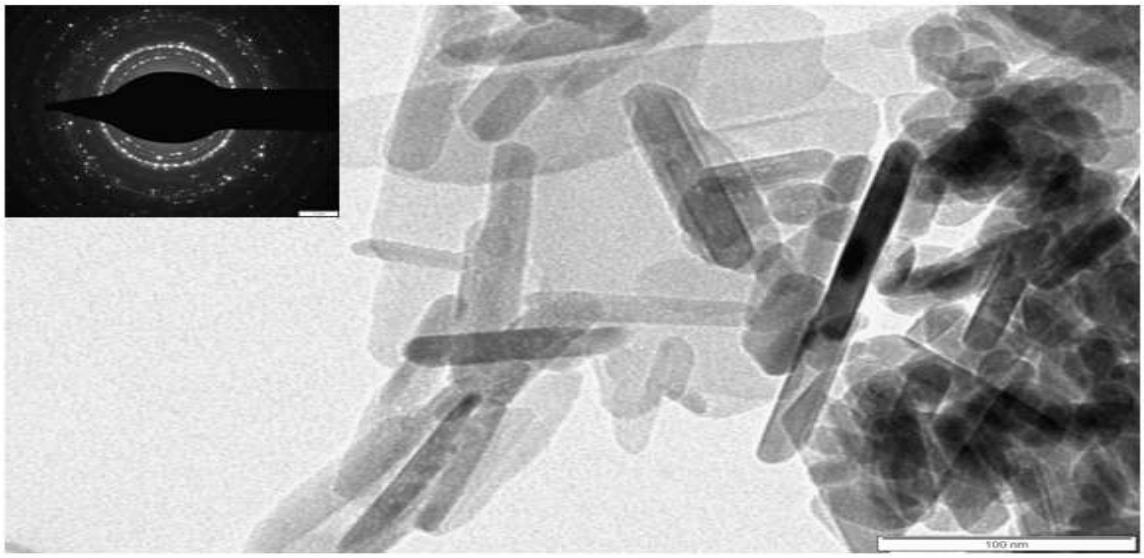


**Fig. 6: TEM image for hydrothermally synthesized hydroxyapatite (HA)**

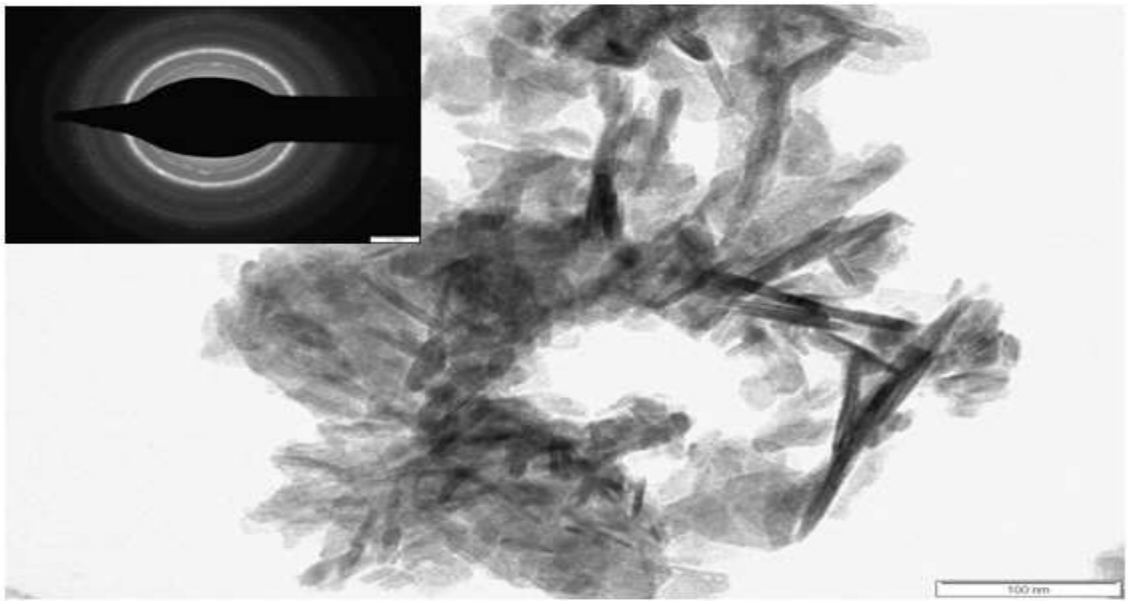


**Fig. 7: TEM image for wet precipitated hydroxyapatite (HA)**

Thermal study of the apatite done via Thermogravimetric/Differential Thermal (TG/DTA) Analysis (Figs. 8 and 9) shows that there was a weight loss of about 6% for temperature up to 380°C and 12% for temperature between 380 to 400ºC, for HA prepared by hydrothermal method and about 9% for temperature up to 220°C and approximately 24% for a range between 220 to 380ºC, for HA prepared by wet precipitation method. Similarly, about 9% weight loss was also observed for temperature up to about 800ºC for HA prepared by hydrothermal method and about 6% weight loss was observed for temperature up to 800ºC for HA prepared by wet precipitation method. In the first stage, an obvious weight loss was observed indicating that there was an evaporation of the absorbed water from the surface and pores (Furedi-Milhofer *et al.*, 1979; Larmas *et al*., 1993). Beyond 800 to 1200ºC, no significant weight loss was observed since an almost stable curve was noticed within this temperature range, suggesting thermal stability of the HA. Since there was no significant weight loss beyond 800 to 1200ºC, it thus supports thermal stability beyond the temperature 1050ºC as proposed for HA by Dean-Mo *et al*. (2002).

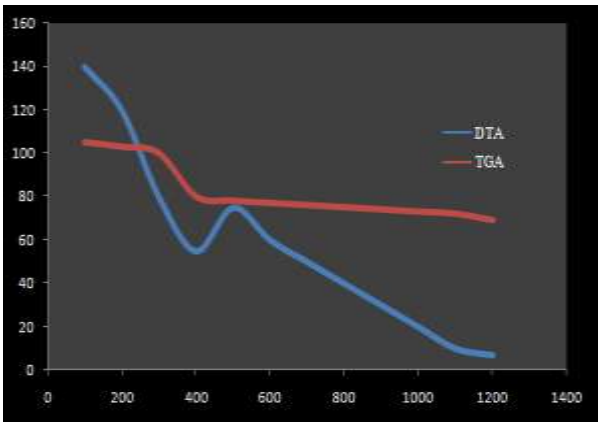


**Fig. 8: TG/DTA curve of HA synthesized via hydrothermal (HT) method**

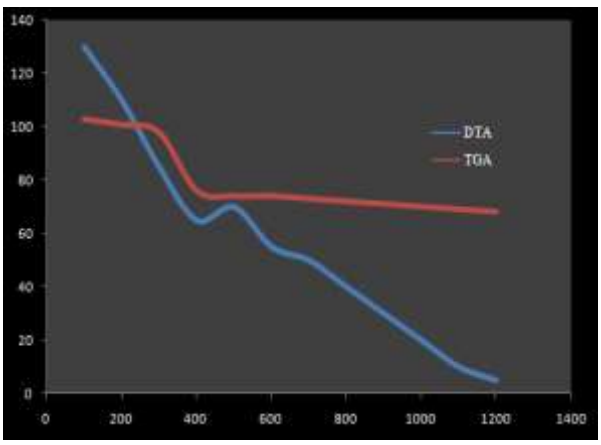


**Fig. 9: TG/DTA curve of HA synthesized via wet precipitation (WT) method**

The DTA curve shows an endothermic sharp peak and broad peak around 400ºC for HA prepared by hydrothermal and wet precipitation methods respectively. This is because removal of water molecules from Calcium nitrate tetrahydrates ($Ca(NO_3)_2.4H_2O$)had occurred, corresponding to physical loss of absorbed water molecules and the removal of crystallized water. Similarly, the endothermic peak at around 600°C in the curve of HA prepared by wet precipitation method is related to the removal of groups like decarboxylation or addition of other groups during the preparation of HA powder. However, the sharp exothermic peaks observed at around 500 and 450ºC for HA prepared by hydrothermal and wet precipitation methods respectively, indicated the crystallization of HA, thus confirming its formation.

**Conclusion**

HA nano-crystals were successful synthesized from the wet precipitation and hydrothermal methods respectively, with the resulting powder from the wet precipitation producing particle in smaller nano regime than the hydrothermal at the physiological conditions employed for these syntheses. As indicated by the results of characterization, XRF/EDX confirms the presence of calcium and phosphorus with Ca/P ratio for both the hydrothermal and wet precipitationshowing good similarity to those of natural bone apatite. FTIR confirms the characteristics bands of the hydroxyapatite (HA), XRD patterns indicated major predominant peaks as HA, as well as confirming its degree of crystallinity ($X_C$) and crystallite size (D), all within the nano regime. Evidences from BET analysis, SEM, TEM all confirmed the morphological and structural properties as being in nano regime while TG/DTA confirms its thermal stability up to 1200ºC which is typical of hydroxyapatite (HA).

**Conflict of Interest**

Authors have declared that there is no conflict of interest in this study.

**References**

Anita LJ, Ravichandran K & Sundareswari M 2015. The study on the synthetic methodologies for manoeuvring the morphology crystalinity and particle size of hydroxyapatite. *J. Chem. and Pharmac. Res.*, 7(2): 231-239.

Cukrov LM, McCormick PG, Galatis K & Wlodarski W 2001. Gas sensing properties of nanosized tin oxide synthesized by mechano-chemical processing. *Sensors and Actuators B. Chemical*, 77(1): 491-495.

Dean-Mo Liu, T Troczynski, Wenjea J Tseng 2001. Water-based sol-gel synthesis ofhydroxyapatite: Process development. *Biomaterials*, 22: 1721-1730.

Elliott JC 1994. Structure and Chemistry of the Apatites and Other Calcium Orthophosphates, *Elsevier*, Amsterdam, p. 111.

Fatehi K, Moztarzadeh F, Soalti-Hashjin M, Tahriri M, Rezvannia M & Ravarian R 2008. *In vitro* biomimetic deposition of apatite on alkaline and heat treated Ti6A14V alloy surface. *Bull. Material Sci.*, 31: 101-108.

Fathi M, Hanifi A & Mortazavi V 2008. Preparation and bioactivity evaluation of bone – like hydroxyapatite nanopowder. *J. Materials Processing Techn.*, 202: 536 – 542.

Feng W, Mu-sen L, Yu-peng L & Sheng-song G 2005. Synthesis and microstructure of hydroxyapatite powders in stimulated body fluid. *Journal of Materials Science*, 40: 2073 – 2076.

Furedi-milhofer H, Hlady V, Baker FS, Beebe RA, Wolejko-wikholm N & Kittelberger JS 1979. Temperature programmed dehydration of Hydroxyapatite. *Journal of Colloid Interface Science*, 70: 1 – 9.

Larmas MA, Hayrynen H & Lajunen LHJ 1993. Thermo gravimetric studies on sound and carious human enamel and dentin as well as hydroxyapatite. *Scandinavian J. Dental Res.*, 101: 185 – 191

Muthusamy P, Kandiah K, Palanisamy M, Venkatachalam R & Palanisami K 2012. Synthesis, characterization and

biological response of magnesium substituted namobioactive glass particles for biomedical applications.*Ceramic International*, 39: 1683-1694.

NejaticE., Firouzdor, V., Eslaminejad, M.B. and Bagheri. (2009). Needle-like Nano hydroxyapatite/poly (L-Lactic acid) Composite Scaffold for Bone tissue engineering application.*Materials Science and Engineering* C, 29, 942-949.

Rajabi-zamani, A. H., Behnamghader, A., kazemzadeh, A. (2008). Synthesis of nano crystalline carbonated hydroxyapatite power via nonalkoxide sol-gel method. *Materials Sci. and Engr*., 28: 1326 – 1329.

Sergent N, Gelin P, Perier-Camby H, Praliaud H & Thomas G 2002. Interaction of water, hydrogen and their mixtures with $SnO_2$ based materials: the role of hydroxyl group in detection mechanism. *Sensors and Actuators B. Chemical*, 84: 176.

Song KC & Kang Y 2000. Preparation of high surface area tin oxide powders by a homogeneous preparation method. *Materials Letters*, 42(5): 283-289.

Toledo-Antonio JA, Baez RG, Sebastian PJ & Vazquez A 2003. Thermal stability and structural deformation of rutile $SnO_2$ nanoparticles. *Journal of Solid State Chemistry*, 174: 241.

Watanabe, T., Kawachig, G., Kamitakahara, M., Kikuta, K and Ohtsuki, C (2009). Formation of needle-like hydroxyapatite by hydrothermal treatment of $CaHPO_4.2H_2O$ combined with $\beta$-$Ca_3(PO_4)_2$. *Journal of the Ceramic Society of Japan*, 117(1366): 759-764.

Young RA & Holcomb DW 1982. Variability of hydroxyapatite preparations. *Calcified Tissue International*, 34: 17–32.

Zhang X & Vecchio KS 2007. Hydrothermal synthesis of hydroxyapatite rods. *Journal of Crystal Growth*, 308: 133 – 140.